Synthesis, Structure, and Reactivity of Group 4 Metallocene Tellurolates. X-ray Crystal Structures of $Cp_2Zr[TeSi(SiMe_3)_3]_2$, $Cp'_2Ti[TeSi(SiMe_3)_3]_2$, $Cp_2Zr(\eta^2\text{-}COMe)[TeSi(SiMe_3)_3]$, and $Cp_2Ti[TeSi(SiMe_3)_3]PMe_3$

Victor Christou, Stephen P. Wuller, and John Arnold*

Contribution from the Department of Chemistry, University of California, Berkeley, California 94720

Received May 4, 1993®

Abstract: Treatment of Cp_2MCl_2 (Cp = η^5-C_5H_5; M = Ti, Zr, Hf) with 2 equiv of $(THF)_2LiTeSi(SiMe_3)_3$ produces the bis-tellurolates $Cp_2M[TeSi(SiMe_3)_3]_2$ (M = Ti (**1**), Zr (**2**), Hf (**3**)) in high yields. For titanium, the Cp′ (Cp′ = η^5-C_5H_4Me) derivative (**4**) was also prepared. The X-ray structures of **2** and **4** were determined and are presented for comparison. Tellurolysis of Cp_2ZrMe_2 with 1 equiv of $HTeSi(SiMe_3)_3$ gave $Cp_2Zr(Me)[TeSi(SiMe_3)_3]$ (**5**); treatment with a second equiv of tellurol produced **2**, again in high yield. Addition of CO to the methyl tellurolate **5** formed the acyl derivative $Cp_2Zr(\eta^2\text{-}COMe)[TeSi(SiMe_3)_3]$ (**6**). Treatment of Cp_2MCl_2 with the alkyltellurolate reagent $(THF)_3LiTeC(SiMe_3)_3$ leads to unstable complexes, $Cp_2M[TeC(SiMe_3)_3]_2$ (M = Ti (**7**), Zr (**8**)), which extrude elemental tellurium between −60 and −20 °C to form alkylmetallocene complexes $Cp_2M[C(SiMe_3)_3]_2$ (M = Ti (**9**),Zr (**10**)); the latter species are unstable at room temperature and subsequently decompose giving the alkane $HC(SiMe_3)_3$ and unidentified metal products. Quantitative reduction to Ti(III) species occurred on addition of Lewis bases to **1** resulting in formation of $Cp_2Ti[TeSi(SiMe_3)_3]L$ (L = PMe_3 (**11**), PEt_3 (**12**), PMe_2Ph (**13**), 2,6-$Me_2C_6H_3NC$ (**14**)). These reduced species were prepared independently from $[Cp_2TiCl]_2$ using $(THF)_2LiTeSi(SiMe_3)_3$ and the appropriate ligand. The X-ray crystal structure of **11** has also been determined. Treatment of **1** with CO gave $[TeSi(SiMe_3)_3]_2$ and $Cp_2Ti(CO)_2$. Reaction of **1** with CO_2 and CS_2 also produced the ditelluride along with the titanium(III) carbonate $\{[Cp_2Ti]_2(CO_3)\}_2$ and the tetrathiolene titanium(IV) complex $[Cp_2Ti]_2(C_2S_4)$, respectively. Crystallographic data for **2**, **4**, **6**, and **11** are as follows. **2**: orthorhombic, *Pnna*, a = 10.320(2) Å, b = 29.828(6) Å, c = 15.200(3) Å, R = 0.0311, R_w = 0.0306. **4**: monoclinic, *C2/c*, a = 28.3996(3) Å, b = 11.0404(4) Å, c = 15.3397(3) Å, β = 93.49(3)°, R = 0.0349, R_w = 0.0511. **6**: monoclinic, $P2_1/c$, a = 31.209(5) Å, b = 13.806(3) Å, c = 13.834(3) Å, β = 91.741(13)°, R = 0.0309, R_w = 0.0355. **11**: monoclinic, $P2_1/c$, a = 18.797(4) Å, b = 13.169(2) Å, c = 25.414(5) Å, β = 91.969(18)°, R = 0.0473, R_w = 0.0432.

Introduction

The recent increase in the number of complexes containing tellurium has been fueled by the interest in soluble metal tellurolate species as single-source precursors to II–VI materials.[1-4] Concomitant with work directed towards the design of such precursors has been work focusing on the mechanistic processes that govern decomposition to the metal tellurides (eq 1).[5]

$$M(TeR)_2 \rightarrow [MTe] + TeR_2 \qquad (1)$$

Thus, recent reports have shown how this decomposition can be thought to occur via terminal telluride species,[6] which might then aggregate to form small clusters on route to formation of the bulk material.[7] To date, however, little is known regarding the reactivity of metal tellurolates. For example, there are few studies that deal with M–Te bond cleavage,[8] despite the fact that these processes necessarily occur in reactions such as those depicted in eq 1. We were interested in studying tellurolate derivatives of the early metals as we hoped that the combination of a hard metal center with a soft, polarizable tellurolate ligand might engender unusual reactivity. Complexes of this type are extremely rare; only a handful of metallocene species such as $Cp_2M(TePh)_2$ (M = Ti, Zr),[9] $Cp_2Ti(Te_2C_6H_4)$,[10] and the recently reported homoleptic derivatives $M[TeSi(SiMe_3)_3]_4$ (M = Ti, Zr, Hf) are known,[6] and almost nothing is known of the structure or reactivity of these compounds. Since the Cp_2M fragment provides a well-defined platform for the study of a wide range of Cp_2ML_2 derivatives, we began the first detailed study of the chemistry of early metal tellurolates based on this ligand system. Here we focus on the preparation and reactivity of a new class of tellurolate derivatives of the general formula $Cp_2M(TeR)_nL_{2-n}$ (M = Ti, Zr, Hf, n = 1, 2).

Results and Discussion

Preparation and Characterization of Metallocene Tellurolates. The silyltellurolates were synthesized in high yields by ligand

* Abstract published in *Advance ACS Abstracts*, October 1, 1993.

(1) See for example: (a) O'Brien, P. *Chemtronics* **1991**, *5*, 61. (b) Brennan, J. G.; Siegrist, T.; Carroll, P. J.; Stuczynski, S. M.; Reynders, P.; Brus, L. E.; Steigerwald, M. L. *Chem. Mater.* **1990**, *2*, 403. (c) Steigerwald, M. L.; Sprinkle, C. R. *J. Am. Chem. Soc.* **1987**, *109*, 7200. (d) Steigerwald, M. L.; Sprinkle, C. R. *Organometallics* **1988**, *7*, 245. (e) Bochmann, M.; Webb, K. J. *J. Chem. Soc., Dalton Trans.* **1991**, 2325. (f) Bochmann, M.; Webb, K. J.; Hursthouse, M. B.; Mazid, M. *J. Chem. Soc., Dalton Trans.* **1991**, 2317 and references in the above.

(2) Bonasia, P. J.; Arnold, J. *Inorg. Chem.* **1992**, *31*, 2508.

(3) Seligson, A. L.; Bonasia, P. J.; Arnold, J.; Yu, K. M.; Walker, J. M.; Bourret, E. D. *Mater. Res. Soc. Symp. Proc.* **1992**, *282*, 665.

(4) Arnold, J.; Walker, J. M.; Yu, K. M.; Bonasia, P. J.; Seligson, A. L.; Bourret, E. D. *J. Cryst. Growth* **1992**, *124*, 674.

(5) Siemeling, U. *Angew. Chem., Int. Ed. Engl.* **1993**, *32*, 67.

(6) Christou, V.; Arnold, J. *J. Am. Chem. Soc.* **1992**, *114*, 6240.

(7) Cary, D. R.; Arnold, J. *J. Am. Chem. Soc.* **1993**, *115*, 2520.

(8) (a) Berry, F. J. In *Comprehensive Coordination Chemistry*; Wilkinson, G., Gillard, R. D., McCleverty, J. A., Eds.; Pergamon: New York, 1987; Vol. 2; Chapter 17. (b) Gysling, H. J. *Coord. Chem. Rev.* **1982**, *42*, 133. (c) Gysling, H. J. In *The Chemistry of Organic Selenium and Tellurium Compounds*; Patai, S., Rappoport, Z., Eds.; Wiley: New York, 1986; Vol. 1; p 679.

(9) Sato, M.; Yoshida, T. *J. Organomet. Chem.* **1974**, *67*, 395.

(10) Köpf, H.; Klapötke, T. *J. Chem. Soc., Chem. Commun.* **1986**, 1192.

0002-7863/93/1515-10545$04.00/0

Table I. Selected Physical and Spectroscopic Data for Cp_2M Silyltellurolates

compd	physical properties	^1H NMR, δ[a]	$^{13}C\{^1H\}$ NMR, δ[a]	$^{125}Te\{^1H\}$ NMR, δ[a]
$Cp_2Ti[TeSi(SiMe_3)_3]_2$ (**1**)	black cryst, mp 181–182 °C	6.07 (s, 10 H), 0.47 (s, 54 H)	111.0, 2.80	810
$Cp_2Zr[TeSi(SiMe_3)_3]_2$ (**2**)	red needles, mp 204–205 °C	6.03 (s, 10 H), 0.47 (s, 54 H)	110.0, 2.39	–26
$Cp_2Hf[TeSi(SiMe_3)_3]_2$ (**3**)	orange cryst, mp 194–195 °C	5.98 (s, 10 H), 0.47 (s, 54 H)	109.2, 2.84	–233
$Cp'_2Ti[TeSi(SiMe_3)_3]_2$ (**4**)	black cryst, mp 183–185 °C	6.62 (t, 2 H), 5.95 (t, 2 H), 1.51 (s, 6 H), 0.29 (s, 54 H)	121.5, 115.1, 111.6, 16.70, 2.90	783
$Cp_2Zr(Me)[TeSi(SiMe_3)_3]$ (**5**)	orange-red plates	5.84 (s, 10 H), 0.45 (s, 27 H), –0.42 (s, 3 H)		–207
$Cp_2Zr(\eta^2\text{-COMe})[TeSi(SiMe_3)_3]$ (**6**)	orange needles, mp 147–150 °C	5.44 (s, 10 H), 2.17 (s, 3 H), 0.55 (s, 27 H)	308.5, 110.0, 31.3, 2.20	–1146

[a] See Experimental Section for conditions, etc.

metathesis using $(THF)_2LiTeSi(SiMe_3)_3$[11,12] and the appropriate metallocene dihalides (eq 2).

$$Cp_2M\begin{matrix}Cl\\Cl\end{matrix} + 2(THF)_2LiTeSi(SiMe_3)_3 \xrightarrow[-2LiCl]{\text{hexanes, 0 °C}} Cp_2M\begin{matrix}TeSi(SiMe_3)_3\\TeSi(SiMe_3)_3\end{matrix} \quad (2)$$

M = Ti (**1**), Zr (**2**), Hf (**3**)

Compounds **1–3** are highly colored, crystalline, air-sensitive solids that are easily purified by recrystallization from hexanes. These reactions are rapid at room temperature and are complete within 4 h. Monitoring the reaction by ^1H NMR spectroscopy shows only formation of the bis-tellurolate. Addition of 1 equiv of lithium tellurolate at –78 °C resulted in formation of 0.5 equiv of $Cp_2M[TeSi(SiMe_3)_3]_2$. The same reaction performed in THF resulted in quantitative reduction of Cp_2TiCl_2 to $[Cp_2TiCl]_2$ concomitant with formation of the ditelluride $[TeSi(SiMe_3)_3]_2$ and LiCl (eq 3).[13]

$$Cp_2TiCl_2 + (THF)_2LiTeSi(SiMe_3)_3 \xrightarrow[-LiCl]{\text{THF, 25 °C}} {}^1/_2[Cp_2TiCl]_2 + {}^1/_2[TeSi(SiMe_3)_3]_2 \quad (3)$$

The tellurolate ligands in **1–3** give rise to a singlet at δ 0.47 ppm in the ^1H NMR spectrum. The cyclopentadienyl resonances show small upfield shifts from δ 6.07 ppm (**1**) to δ 6.03 ppm (**2**) and δ 5.98 ppm (**3**). This trend is seen far more emphatically in the $^{125}Te\{^1H\}$ NMR spectra (Table I) where the resonances are separated by more than 1000 ppm (**1**, δ 810 ppm; **2**, δ –26 ppm; **3**, δ –232 ppm) reflecting changes in the electrophilicity and electron polarizability of the respective metal centers.[14] In addition to the usual electronic absorptions associated with d^0 metallocenes, the spectra of **1–3** show weak, low-energy ligand-to-metal charge-transfer bands that shift hypsochromically upon descending the group (**1**, 810 nm; **2**, 528 nm; **3**, 474 nm).

As crystals of **1** were unsuitable for X-ray diffraction studies, the analogous MeCp derivative $(\eta^5\text{-}C_5H_4Me)_2Ti[TeSi(SiMe_3)_3]_2$ (**4**) was prepared.[15] We have structurally characterized both **4** and **2** as shown in Figures 1 and 2, respectively. Data collection and metrical parameters can be found in Tables II and III. These

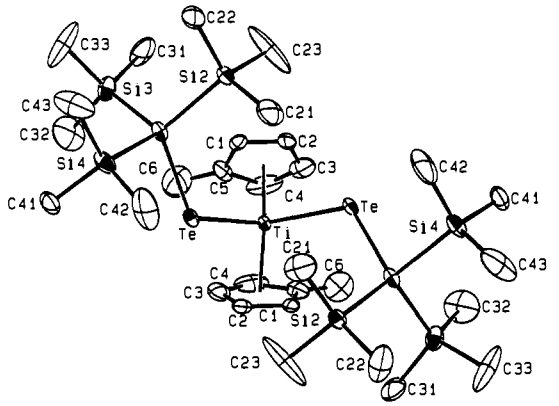

Figure 1. ORTEP View of $(\eta^5\text{-}C_5H_4Me)_2Ti[TeSi(SiMe_3)_3]_2$ (**4**).

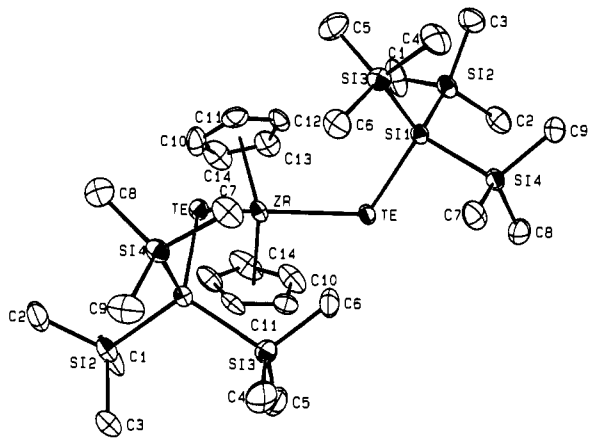

Figure 2. ORTEP View of $Cp_2Zr[TeSi(SiMe_3)_3]_2$ (**2**).

are the first X-ray crystallographic studies of metallocene tellurolate species.

Both structures have crystallographically imposed 2-fold axes and pseudotetrahedral symmetry about the metal; however, due to the steric bulk of the tellurolate ligands the metals show severe distortions away from tetrahedral symmetry. Thus, the Te–Zr–Te bond angle of **2** is extremely large (106.32°) compared to other substituted Cp_2ZrL_2 species.[14] The ZrTe bond length, 2.866 Å, is close to the sum of calculated covalent radii (Σ_{Zr-Te} = 2.86 Å).[16] For comparison, in the isoelectronic species $Zr(Te)[TeSi(SiMe_3)_3]_2(dmpe)_2$ the Zr–TeR bond lengths are 2.939 and 3.028 Å and in the (formally) 8-electron homoleptic complex $Zr[TeSi(SiMe_3)_3]_4$ the mean value is 2.735 Å.[6] The structure of **4** is also characterized by an unusually large Te–M–Te bond angle (99.42°), compared to the usual angle of around 95° seen in

(11) Bonasia, P. J.; Gindleberger, D. E.; Dabbousi, B. O.; Arnold, J. *J. Am. Chem. Soc.* **1992**, *114*, 5209.

(12) For related work on derivatives of this ligand see: Becker, G.; Klinkhammer, K. W.; Lartiges, S.; Böttcher, P.; Poll, W. *Z. Anorg. Allg. Chem.* **1992**, *613*, 7. Uhl, W.; Layh, M.; Becker, G.; Klinkhammer, K. W.; Hildenbrand, T. *Chem. Ber.* **1992**, *125*, 1547. Becker, G.; Klinkhammer, K. W.; Schwarz, W.; Westerhausen, M.; Hildenbrand, T. *Z. Naturforsch. B.* **1992**, *47*, 1225.

(13) Reduction of Ti(IV) is quite facile. See for example: Atwood, J. L.; Barker, G. K.; Holton, J.; Hunter, W. E.; Lappert, M. F.; Pearce, R. *J. Am. Chem. Soc.* **1977**, *99*, 6645.

(14) Cardin, D. J.; Lappert, M. F.; Raston, C. L. *Chemistry of Organo-Zirconium and -Hafnium Compounds*; Ellis-Horwood: Chichester, 1986.

(15) See the following references for use of methylcyclopentadienyl derivatives as crystallographic "locks" in determination of crystal structures: (a) Petersen, J. L.; Dahl, L. *J. Am. Chem. Soc.* **1974**, *96*, 2248. (b) Petersen, J. L.; Dahl, L. F. *J. Am. Chem. Soc.* **1975**, *97*, 6422.

(16) The average covalent radii of titanium (Ti(IV) = 1.44 Å, Ti(III) = 1.47 Å) and zirconium (1.50 Å) were calculated by subtracting the covalent radius of carbon (0.771 Å) from published σ bond length data for M–R (M = Ti, Zr) in metallocene complexes. The covalent radius of tellurium (1.358 Å) was calculated from structural data for $-TeSi(SiMe_3)_3$ over a range of crystallographically characterized tellurolate complexes.

Table II. Crystallographic Data

	2	4	6	11
formula	$ZrTe_2Si_8C_{28}H_{64}$	$TiTe_2Si_8C_{30}H_{68}$	$ZrTeSi_4OC_{21}H_{40}$	$TiTePSi_4C_{22}H_{46}$
mol wt, amu	971.9	956.7	639.7	629.4
cryst size, mm	0.14 × 0.22 × 0.31	0.15 × 0.30 × 0.35	0.12 × 0.37 × 0.47	0.15 × 0.15 × 0.38
space group	*Pnna*	*C*2/*c*	$P2_1/c$	$P2_1/c$
a, Å	10.320(2)	28.3996(3)	31.209(5)	18.797(4)
b, Å	29.828(6)	11.0404(4)	13.806(3)	13.169(2)
c, Å	15.200(3)	15.3397(3)	13.834(3)	25.414(5)
α, deg	90.0	90.0	90.0	90.0
β, deg	90.0	93.49(3)	91.741(13)	91.969(18)
γ, deg	90.0	90.0	90.0	90.0
V, Å^3	4678.7(27)	4800(3)	5958.4(31)	6287.4(35)
Z	4	4	8	8
d_{calcd}, g cm^{-3}	1.38	1.32	1.43	1.33
radiation, Å	Mo Kα 0.71073	Mo Kα 0.71073	Mo Kα 0.71073	Mo Kα 0.71073
scan mode	Ω	θ–2θ	Ω	Ω
2θ range, deg	3–45	3–45	3–45	3–45
collection range	$+h,+k,\pm l$	$+h,+k,\pm l$	$+h,+k,\pm l$	$+h,+k,\pm l$
abs coeff (μ), cm^{-1}	16.7	15.9	14.9	13.9
no. of reflns coll	6649	3418	8514	8644
no. of unique reflns	3052	3141	7755	8204
reflns w/$F^2 > 3\sigma(F^2)$	2062	2726	6172	3189
final R, R_w	0.0311, 0.0306	0.0349, 0.0511	0.0309, 0.0355	0.0473, 0.0432
T, °C	−108	−100	−110	−98

Table III. Selected Bond Distances and Angles for **2** and **4**

	$TiTe_2Si_8C_{30}H_{68}$ (**4**)	$ZrTe_2Si_8C_{28}H_{64}$ (**2**)
	Intramolecular Distances, Å	
M–Te	2.788(1)	2.866(1)
$(M–C)_{av}$	2.360(6)	2.501(7)
M–Cp(centroid)	2.042(1)	2.202(1)
Te–Si	2.526(2)	2.521(2)
$(Si–Si)_{av}$	2.355(2)	2.352(2)
	Intramolecular Angles, deg	
Te–M–Te	99.42(4)	106.32(3)
Cp–M–Te	109.8	98.71
Cp–M–Te	109.3	110.07
Cp–M–Cp	132.9	131.29
M–Te–Si1	121.42(4)	123.32(4)
Te–Si1–Si2	115.48(7)	113.03(8)
Te–Si1–Si3	114.60(8)	114.61(8)
Te–Si1–Si4	97.67(7)	98.21(8)

other titanocene structures.[17] This distortion is again attributed predominantly to the steric bulk of the tellurolate ligand. Similarly, the Ti–Te bond length of 2.788 Å is close to that expected on the basis of the sum of covalent radii (Σ_{Ti-Te} = 2.80 Å).[16] Bond angles and lengths within the tellurolate ligand itself are similar for both structures and show the same distortions often seen in the structures of other crystallographically characterized tris(trimethylsilyl)silyltellurolate complexes, the most notable being the slight distortion away from tetrahedral symmetry of the central silicon atom in the ligand.[2,6,7,11,18]

Tellurolysis provides an alternative but equally effective pathway to early-transition-metal metallocene tellurolates. Thus, reaction of Cp_2ZrMe_2 with 2 equiv of $HTeSi(SiMe_3)_3$[11] in hexanes at 50 °C for 3 h affords high yields of **2** and methane (eq 4).

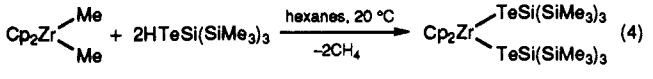

(4)

2

Addition of only 1 equiv of tellurol at 20 °C results in protonation of a single Zr–Me bond and formation of the orange-red methyl tellurolate complex, **5** (eq 5). The latter is immensely soluble in

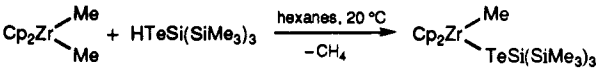

(5)

5

hexane and purification by crystallization is difficult, even at −80 °C. Although **5** could not be obtained in analytically pure form, its identity was confirmed by reaction with CO (3 atm) in hexanes, which gave bright orange needles of the less soluble 18-electron acyl species $Cp_2Zr(\eta^2\text{-COMe})[TeSi(SiMe_3)_3]$ (**6**) (eq 6).

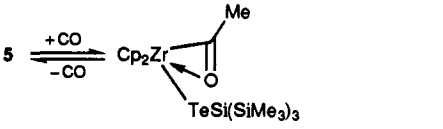

(6)

6

Compound **6** crystallizes from diethyl ether in good yields and is stable in the solid state under nitrogen for months. Insertion of CO is reversible, nonetheless, and dissolution results in slow extrusion of CO with clean regeneration of **5**. The acyl shows a strong ν_{CO} at 1551 cm^{-1}, a value which is at the high end of the range seen for other zirconocene acyls,[19] while the $^{13}C\{^1H\}$ NMR shift of the carbonyl carbon atom (δ 308.5 ppm) falls within the range reported for other zirconium acyl species. The most notable feature in the ^1H NMR spectrum is the acyl resonance at 2.17 ppm which is shifted nearly 2.5 ppm downfield from the methyl resonance of **5**, reflecting the increased electron density at the metal.

Isolation of this material in crystalline form allows for comparison of the Zr–Te bonds length in this 18-electron species with that described for the 16-electron bis-tellurolate **2** described above. The molecular structure of **6** is shown in Figure 3 with crystal and data collection parameters summarized in Table II; Table IVlists selected bond angles and lengths. The structure consists of two independent molecules in the asymmetric unit with no abnormally close contacts between individual molecules. Each molecule has the acyl ligand coordinated η^2 across the CO bond to the Zr atom and an approximate non-crystallographic mirror plane along the Zr–Te–Si plane. The major difference

(17) For examples of typical Cp_2TiL_2 type structures see: (a) Davis, B. R.; Bernal, I. *J. Organomet. Chem.* **1971**, *30*, 75. (b) Epstein, E. F.; Bernal, I.; Köpf, H. *J. Organomet. Chem.* **1971**, *26*, 229. (c) Epstein, E. F.; Bernal, I. *Inorg. Chim. Acta* **1973**, *7*, 211. (d) Bottomley, F.; Lin, I. J. B.; White, P. S. *J. Organomet. Chem.* **1981**, *212*, 341. (e) Kockman, V.; Rucklidge, J. C.; O'Brien, R. J.; Santo, W. *J. Chem. Soc., Chem. Commun.* **1971**, 1340.

(18) Gindelberger, D. E.; Arnold, J. *J. Am. Chem. Soc.* **1992**, *114*, 6242.

(19) Campion, B. K.; Falk, J.; Tilley, T. D. *J. Am. Chem. Soc.* **1987**, *109*, 2049.

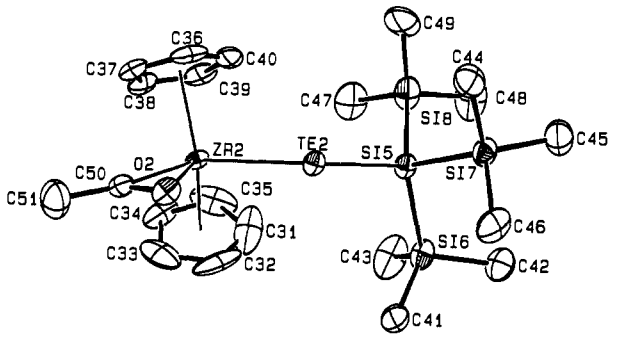

Figure 3. ORTEP View of $Cp_2Zr(\eta^2\text{-COMe})[TeSi(SiMe_3)_3]$ (6).

Table IV. Selected Bond Distances and Angles for 6

molecule 1		molecule 2	
	Intramolecular Distances, Å		
Zr1–Te1	2.990(1)	Zr2–Te2	2.996(1)
Zr1–O1	2.284(3)	Zr2–O2	2.296(3)
Zr1–C20	2.176(5)	Zr2–C50	2.187(5)
C20–O1	1.236(6)	C50–O2	1.246(6)
C20–C21	1.491(8)	C50–C52	1.477(8)
$(Zr1–C)_{av}$	2.494(5)	$(Zr2–C)_{av}$	2.491(5)
Zr1–Cp1	2.205	Zr2–Cp3	2.199
Zr1–Cp2	2.196	Zr2–Cp4	2.201
Te1–Si1	2.510(1)	Te2–Si5	2.502(1)
	Intramolecular Angles, deg		
Te1–Zr1–O1	74.18(19)	Te2–Zr2–O2	75.16(9)
Te1–Zr1–C20	106.15(15)	Te2–Zr2–C50	107.31(15)
Te1–Zr1–Cp1	105.22	Te2–Zr2–Cp3	106.80
Te1–Zr1–Cp2	108.15	Te2–Zr2–Cp4	105.76
O1–Zr1–Cp1	113.23	O2–Zr2–Cp3	111.12
O1–Zr1–Cp2	110.14	O2–Zr2–Cp4	112.13
C20–Zr1–Cp1	102.36	C50–Zr2–Cp3	102.15
C20–Zr1–Cp2	101.97	C50–Zr2–Cp4	102.05
Cp1–Zr1–Cp2	130.70	Cp3–Zr2–Cp4	130.87
Zr1–C20–O1	78.8(3)	Zr2–C50–O2	78.7(3)
Zr1–C20–C21	160.6(4)	Zr2–C50–C51	159.9(4)
O1–C20–C21	120.4(5)	O2–C50–C51	121.3(5)
Zr1–Te1–Si1	120.66(4)	Zr2–Te2–Si5	119.44(4)
Te1–Si1–Si2	104.55(6)	Te2–Si5–Si6	114.77(7)
Te1–Si1–Si3	104.18(7)	Te2–Si5–Si7	99.99(6)
Te1–Si1–Si4	120.01(7)	Te2–Si5–Si8	113.26(7)

between the two molecules in the asymmetric unit is the orientation of the $Si(3)Me_3$ group in the tellurolate ligand relative to the Te–Zr bond. In molecule 1 this group is *cis* to the Te–Zr bond, whereas in molecule 2 the $Si(3)Me_3$ group is *trans* to the corresponding bond. This conformational change has little effect on the bond distances and angles about the metal center influencing primarily the angles around the central Si atom of the bulky ligand, which are dramatically different between the two molecules. The structure shows several characteristic distortions that are typical of zirconium acyl species.[19] Thus, the Zr–C bond length is significantly shortened, the C–O bond length is slightly elongated, and the angles are more in line with triangular η^2-coordination of the acyl-to-Zr rather than normal sp^2 geometry. Significantly, the Zr–Te bond length (2.990 Å) is much longer than the corresponding bond length in **2** (2.880 Å).

Attempts to prepare and isolate the *alkyl*tellurolates, $Cp_2M[TeC(SiMe_3)_3]_2$ (M = Ti (**7**), Zr (**8**)), via metathesis from Cp_2MCl_2 with $(THF)_3LiTeC(SiMe_3)_3$[20] failed. The only isolated products were elemental tellurium and the alkane $HC(SiMe_3)_3$. Monitoring the reaction at −60 °C by ^1H NMR spectroscopy indicated that **8** was formed [δ 5.89 (s, 10 H), 0.51 (s, 54 H)]; however, upon warming to −20 °C decomposition occurred by extrusion of elemental tellurium to form $Cp_2Zr[C(SiMe_3)_3]_2$ (**10**) (Scheme I).

(20) Sladky, F.; Bildstein, B.; Rieker, C.; Gieren, A.; Betz, H.; Hubner, T. *J. Chem. Soc., Chem. Commun.* **1985**, 1800.

Scheme I

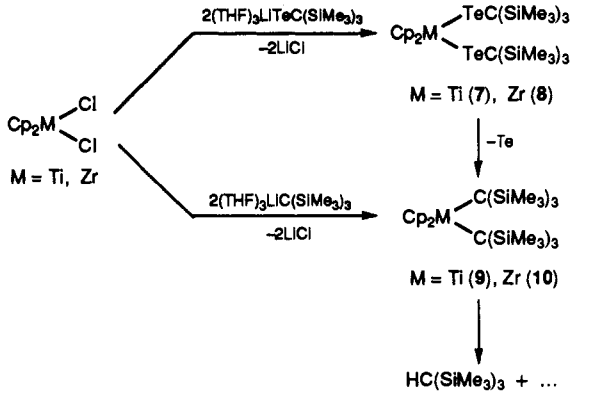

Compound **10** was prepared independently from Cp_2ZrCl_2 and 2 equiv of $(THF)_3LiC(SiMe_3)_3$; however, this material is itself unstable above ca. −20 °C, decomposing to alkane and unidentified metal-containing species. The corresponding titanocene tellurolate, **7**, is even more labile and was never observed even at −60 °C. The major products from this reaction were elemental tellurium and alkane. NMR data showed the alkyltitanocene $Cp_2Ti[C(SiMe_3)_3]_2$ (**9**) was much less stable than **10**, and again the only characterizable product was the alkane. In forming the latter, no evidence was found for deuterium abstraction from the solvent, suggesting that the cyclopentadienyl rings are the source of the alkane C–*H* in these reactions.

It is interesting to note that these results support our general observation that silyl chalcogenolates appear to form metal complexes that are more thermally stable than their alkyl counterparts.[2-4,6,7,11,21] There are two factors that may be responsible for this differing stability: (i) Te–Si bonds are ca. 10 kcal mol^{-1} stronger than Te–C bonds,[22] and (ii) the smaller radius of C (and, therefore, the shorter Te–C bond length) may lead to increased intra- and interligand repulsions that serve to destabilize already crowded coordination geometries.

Reactivity of 1. Compound **1** is unstable in hydrocarbon solutions at 20 °C, decomposing over prolonged periods to a mixture of ditelluride and uncharacterized Ti products. This decomposition was noticeably faster in dilute solutions, such that a 10^{-4} M solution of **1** in hexanes had decomposed completely within 12 h. The EPR spectra of samples of **1** in MCH (MCH = methylcyclohexane, 10^{-3} M) prepared in the dark showed two very weak signals at 298 K: a sharp isotropic singlet (g_{iso} = 1.9800) and a broader singlet at lower field (g_{iso} = 2.38, $\Delta H_{1/2}$ = 400 G).[23] Suspecting the involvement of an equilibrium of the kind shown in eq 7,

$$1 \rightleftharpoons Cp_2Ti[TeSi(SiMe_3)_3] + (Me_3Si)_3SiTe^{\bullet} \quad (7)$$

we conducted trapping experiments with Lewis bases of varying basicity and steric bulk (eq 8).

$$1 \xrightarrow[\text{hexanes, 25 °C}]{L} Cp_2Zr\begin{matrix}TeSi(SiMe_3)_3\\ L\end{matrix} + {}^1/_2[TeSi(SiMe_3)_3]_2 \quad (8)$$

L = PMe_3 (**11**), PEt_3 (**12**), PMe_2Ph (**13**), 2,6-$Me_2C_6H_3NC$ (**14**)

These reactions were generally complete within 4 h at room temperature in the dark, and the paramagnetic Ti(III) products were isolated as crystalline solids in moderate to high yields. The ditelluride byproduct was removed by washing with cold hexamethyldisiloxane, leaving pure **11–14** as purple or red/brown

(21) Bonasia, P. J.; Arnold, J. *J. Chem. Soc., Chem. Commun.* **1990**, 1299.

(22) $D°_{Te-Si}$ = 122 kcal mol^{-1}; $D°_{Te-C}$ = 110 kcal mol^{-1}. See: (a) Cottrell, T. L. *Strengths of Chemical Bonds*; Butterworths: London. 1958. (b) Mills, K. C. *Thermodynamic Data for Inorganic Sulphides, Selenides and Tellurides*; Butterworths: London. 1974.

(23) Conversion factor: 1 G = 10^{-4} T.

powders. These extremely air and moisture sensitive compounds are immensely soluble in hydrocarbons but can be crystallized from concentrated pentane at −40 °C. The choice of ligand is critical, as only small, relatively basic ligands result in pure isolable titanium(III) products. For example, PMe_3 forms a stable complex while bulkier phosphines such as PPh_3 and PCy_3 or the poor σ-donor $P(OMe)_3$ fail to react. Ligands such as PMe_2Ph, which are still good donors but relatively bulky, appear to be marginal ligands; the isolated products are often contaminated with small amounts of **1**, indicative of incomplete reactions or competitive reactions with the tellurolate radical. These results can be rationalized on the basis of a competition reaction involving either (i) entrapment of the Ti(III) species by L to form **11–14** or (ii) recombination of the tellurolate radical with the Ti(III) species to regenerate **1**. These reductions stop at the Ti(III) stage and, even in the presence of large excesses of either PMe_3 or 2,6-$Me_2C_6H_3NC$, no further reduction to the known Ti(II) species Cp_2TiL_2 occurred.[24,25]

Attempts to prepare the putative 15-electron, titanium(III) species $Cp_2Ti[TeSi(SiMe_3)_3]$ by reaction of $[Cp_2TiCl]_2$ with $(THF)_2LiTeSi(SiMe_3)_3$ were unsuccessful; the only isolated product was the titanium(IV) species **1**. In fact, traces of **1** were frequently observed in much of the Ti(III) chemistry described here, suggesting that disproportionation reactions are facile in these systems. We note that related Ti(III) → Ti(IV/II) disproportionations are well documented.[26] Repeating the reaction in the presence of base, however, resulted in formation of the titanium(III) monotellurolates **11–14**, again in high yields. An alternative route to the same species was effected by reaction of Cp_2TiCl_2 with 2 equiv of $(THF)_2LiTeSi(SiMe_3)_3$ in THF in the presence of the required base. Thus, reaction of Cp_2TiCl_2 with $(THF)_2LiTeSi(SiMe_3)_3$ in THF in the presence of PMe_3 resulted in near quantitative formation of **11** within 5 min.

All Ti(III) species have been characterized by a combination of spectroscopic, magnetic susceptibility and elemental analysis data and in the case of the PMe_3 derivative by X-ray crystallography. EPR spectra of the Ti(III) complexes **11** and **14** were recorded in MCH at 298 K. The main feature in the spectrum of **11** is a doublet (g_{iso} = 2.010) with coupling to ^{31}P of a similar magnitude to that observed in related complexes ($a_{iso}(^{31}P)$ = 20 G).[27] In addition, however, we also detected weaker resonances (see Figure 4a) that we ascribe to Ti hyperfine coupling, again on the basis of the similarity of our data to those of related Cp_2-Ti(III) species[28] ($a_{iso}(^{47/49}Ti)$ = 10 G (^{47}Ti, $I = {}^5/_2$, 7.5 %; ^{49}Ti, $I = {}^7/_2$, 5.5%)). The spectrum of **14** (Figure 4b) shows a broad singlet (g_{iso} = 2.027) with no measurable hyperfine coupling.

The molecular structure of **11** consists of two crystallographically independent molecules, one of which is shown in Figure 5. Crystal data collection and metrical parameters are collected in Tables II and V. Bond distances and angles are similar between both molecules, but torsion angles differ significantly. As expected the Ti–centroid distances, 2.055–2.086 Å, are slightly longer than in **4**, but almost identical to those seen for the only other example of a structurally characterized $Cp_2Ti(PMe_3)L$ (L = $SiHPh_2$) species of this general type.[29] The bond lengthening seen for the Ti–Te bond (Σ_{Ti-Te} = 2.83 Å),[16] 2.912 and 2.879 Å (compared to 2.788 Å in **4**), is likewise attributable to the extra electron in the Ti(III) species. The Ti–P bond distances (2.592 and 2.589 Å) are comparable to those seen in $Cp_2Ti(PMe_3)SiHPh_2$.[29] The

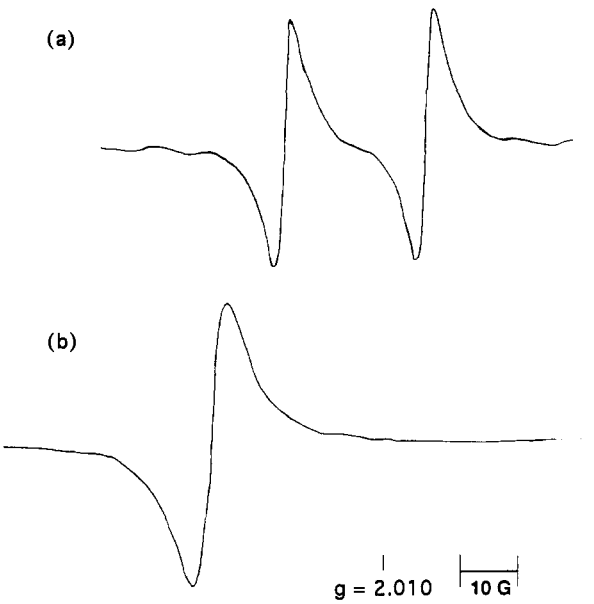

Figure 4. EPR Spectra of **11** (a) and **14** (b) in MCH at 9.2323 GHz (T = 298 K).

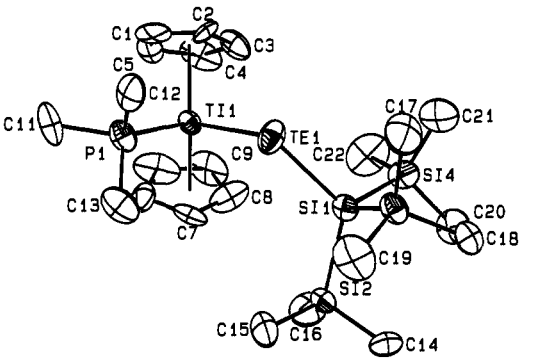

Figure 5. ORTEP View of $Cp_2Ti[TeSi(SiMe_3)_3]PMe_3$ (**11**).

Table V. Selected Bond Distances and Angles for 11

molecule 1		molecule 2	
	Intramolecular Distances, Å		
Ti1–Te1	2.912(3)	Ti2–Te2	2.879(3)
Ti1–P1	2.592(5)	Ti2–P2	2.589(5)
Ti1–C_{av}	2.366(16)	Ti2–C_{av}	2.370(15)
Ti1–Cp1	2.057	Ti2–Cp3	2.063
Ti1–Cp2	2.086	Ti2–Cp4	2.055
Te1–Si1	2.504(4)	Te2–Si5	2.500(4)
Si1–Si2	2.365(6)	Si5–Si6	2.343(6)
Si1–Si3	2.348(6)	Si5–Si7	2.348(6)
Si1–Si4	2.328(6)	Si5–Si8	2.340(6)
P1–C11	1.817(16)	P2–C41	1.833(18)
P1–C12	1.771(17)	P2–C42	1.805(15)
P1–C12	1.798(17)	P2–C43	1.845(13)
	Intramolecular Angles, deg		
Te1–Ti1–P1	80.41(12)	Te2–Ti2–P2	82.30(12)
Te1–Ti1–Cp1	105.76(11)	Te2–Ti2–Cp3	103.80(11)
Te1–Ti1–Cp2	105.52(10)	Te2–Ti2–Cp4	112.05(10)
P1–Ti1–Cp1	106.33(15)	P2–Ti2–Cp3	107.17(14)
P1–Ti1–Cp2	106.36(14)	P2–Ti2–Cp4	104.86(14)
Cp1–Ti1–Cp2	137.69(13)	Cp3–Ti2–Cp4	134.33(13)
Ti1–Te1–Si1	120.45(11)	Ti2–Te4–Si5	122.35(11)
Te1–Si1–Si2	121.65(22)	Te2–Si5–Si6	116.02(19)
Te1–Si1–Si3	100.68(19)	Te2–Si5–Si7	98.47(17)
Te1–Si1–Si4	109.74(18)	Te2–Si5–Si8	113.30(20)

Te–Ti–P angles (80.41° and 82.30°) show characteristic bond angle reductions associated with Ti(III) species. This reduction is no doubt due to a combination of relief of steric strain resulting from loss of one tellurolate ligand and placement of the un-

(24) Kool, L. B.; Rausch, M. D.; Alt, H. G.; Engelhardt, H. E.; Heberhold, M. *J. Organomet. Chem.* **1986**, *317*, C38.
(25) Kool, L. B.; Rausch, M. D.; Alt, H. G.; Heberhold, M.; Thewalt, U.; Wolf, B. *Angew. Chem., Int. Ed. Engl.* **1985**, *24*, 394.
(26) Van Raaij, E. U.; Schmulbach, C. D.; Brintzinger, H. H. *J. Organomet. Chem.* **1987**, *328*, 275.
(27) Samuel, E.; Harrod, J. F.; Gourier, D.; Dromzee, Y.; Robert, F.; Jeannin, Y. *Inorg. Chem.* **1992**, *31*, 3252.
(28) Mach, K.; Raynor, J. B. *J. Chem. Soc., Dalton Trans.* **1992**, 683.
(29) Samuel, E.; Mu, Y.; Harrod, J. F.; Dromzee, Y.; Jeannin, Y. *J. Am. Chem. Soc.* **1990**, *112*, 3435.

paired electron in the stereochemically active, antibonding, a_1 orbital.[15b,30,31] Steric congestionis also minimized by pseudoalignment of one methyl group of the trimethylphosphine in the Te–Ti–P plane, thereby minimizing interaction with the Cp rings. As with structures **2** and **4**, bond angles and lengths within the tellurolate ligand are unremarkable and conform to the typical values seen in other $-TeSi(SiMe_3)_3$ structures.[2,6,11,18,21,32]

We have also briefly examined the reactivity of **1–3** toward small molecules in order to compare their reactivity with that of other Cp_2M derivatives. Treatment of **1** with CO (1 atm, 25 °C) in hexanes resulted in a gradual color change to dark green accompanied by formation of $Cp_2Ti(CO)_2$ and the ditelluride $[TeSi(SiMe_3)_3]_2$. This reaction is quantitative as judged by ^1H NMR spectroscopy and is complete within 12 h.

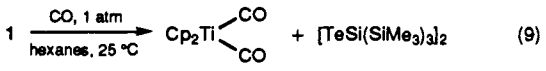

(9)

Increasing the pressure of CO or elevating the temperature accelerates the reaction rate so that at 3 atm and 60 °C the reaction is complete within 2 h. The only species present in the reaction mixture, as judged by ^1H NMR spectroscopy, are **1**, $Cp_2Ti(CO)_2$, and $[TeSi(SiMe_3)_3]_2$; the putative Ti(III) species $Cp_2Ti[TeSi(SiMe_3)_3](CO)$ was not observed. $Cp_2Ti(CO)_2$ was identified by comparison of its spectral data with the literature.[33]

In contrast, **2** and **3** are unreactive toward CO (60 °C, 14 days, 5 atm). This difference presumably reflects the marked difference in redox potentials of Zr and Hf(IV) compared to that of Ti.[14] Similarly, **2** and **3** failed to react with all other substrates described.

Reaction of **1** with CO_2 (1 atm, 60 °C, 36 h) again resulted in the formation of $[TeSi(SiMe_3)_3]_2$ (1 equiv). The Ti(III) species $[(Cp_2Ti)_2(CO_3)]_2$[34] and CO (identified by reaction with Cp_2V) were also produced.

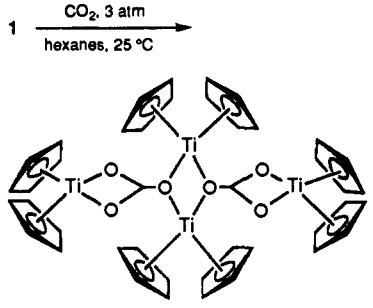

(10)

Reaction of **1** with CS_2 (either neat or as a solution in hydrocarbons) produced $[TeSi(SiMe_3)_3]_2$ and a precipitate of the previously reported Ti(IV) species $[(Cp_2Ti)_2(C_2S_4)]$[35] quantitatively.

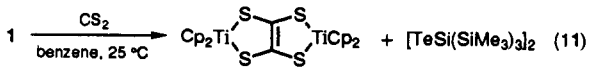

(11)

The tetrathiolene complex was identified by EI/MS and X-ray crystallography.[36]

Summary and Conclusions

Stable bis-silyltellurolate derivatives of early-transition-metal metallocenes have been prepared by both metathetical and tellurolysis routes. The analogous bis-alkyl derivatives are unstable, and this feature is attributed to a combination of a weaker Te–E bond and an increase in steric congestion upon substitution of Si for C. Unlike the zirconocene and hafnocene silyltellurolate derivatives, the titanocene species is photolytically unstable in solution. Isolable Ti(III) species, $Cp_2Ti[TeSi(SiMe_3)_3]L$, can be trapped in near-quantitative yields on reaction with strong, unhindered Lewis bases; the authenticity of these products was confirmed by independent syntheses from $[Cp_2TiCl]_2$ and $(THF)_2LiTeSi(SiMe_3)_3$ in the presence of the respective base. Treatment of the Ti(IV) bis-silyltellurolate with other reagents such as CO, CO_2, and CS_2 results in behavior which mimics that of ligand stabilized titanocene. Whether this occurs via concerted reductive elimination of ditelluride or via a stepwise elimination of tellurolate radicals is as yet unclear and clearly merits further investigation.

Experimental Section

Inert atmosphere glovebox and Schlenk-line techniques were used throughout the preparative procedures. Tetrahydrofuran, diethyl ether, hexanes, benzene, pentane, hexamethyldisiloxane, MCH, and toluene were all predried over 4Å molecular sieves and, with the exception of toluene, distilled from sodium/benzophenone under N_2; toluene was distilled from sodium under N_2. Dichloromethane and acetonitrile were predried over 4Å sieves and distilled from calcium hydride under N_2. All NMR solvents were dried as their undeuterated counterparts, but were purified by vacuum transfer. Cp_2MCl_2 [M = Ti (Aldrich), Zr, Hf (Boulder Scientific)] compounds were used without further purification. Published procedures were used to prepare $Cp_2Ti(CO)_2$,[33] $Cp_2Ti(PMe_3)_2$,[25] Cp_2ZrMe_2,[37] Cp_2V,[38] $[Cp_2TiCl]_2$,[39] $(THF)_2LiTeSi(SiMe_3)_3$,[11] and $HTeSi(SiMe_3)_3$.[11] 2, 6-Me_2ArNC (Fluka) was used as received. PEt_3 (Strem) and PPh_3 (Aldrich) were used as received. PMe_3,[40] PMe_2Ph,[41] and dmpe[42] were prepared by literature procedures. Carbon monoxide and carbon dioxide (bone dry) were used directly from the cylinder. Carbon disulfide (Fison) was dried over calcium hydride and distilled under nitrogen.

Melting points were determined in sealed capillary tubes under nitrogen and are uncorrected. IR samples, unless stated otherwise, were prepared as Nujol mulls between CsI or KBr plates. Electronic spectra were recorded in 0.5-cm quartz cells. Elemental analyses and EI/MS measurements were performed within the College of Chemistry, University of California, Berkeley.

All ^1H NMR spectra were recorded in C_6D_6 at 20 °C, unless otherwise noted. $^{13}C\{^1H\}$ NMR spectra were recorded at ambient temperature at 100.61 MHz. Chemical shifts (δ) for ^1H NMR and $^{13}C\{^1H\}$ NMR spectra are reported relative to residual solvent peak. $^{31}P\{^1H\}$ NMR spectra were recorded in C_6D_6 at ambient temperature at 161.98 MHz. Chemical shifts are relative to external H_3PO_4 at 0 ppm. $^{125}Te\{^1H\}$ NMR samples were prepared as concentrated solutions in 5-mm NMR tubes sealed with rubber septa under dinitrogen. The spectra were recorded at ambient temperature, unless stated otherwise, using one of the following instruments: a Bruker AM 500 spectrometer equipped with a broad band probe operating at 157.90 MHz, a Bruker AMX 400 spectrometer with an inverse broad band probe operating at 126.24 MHz, or a Bruker AMX

(30) Prout, K.; Cameron, T. S.; Forder, R. A.; Critchley, S. R.; Denton, B.; Rees, G. V. *Acta Crystallogr.* **1974**, *B30*, 2290.
(31) Lauher, J. W.; Hoffmann, R. *J. Am. Chem. Soc.* **1976**, *98*, 1729.
(32) Dabbousi, B. O.; Bonasia, P. J.; Arnold, J. *J. Am. Chem. Soc.* **1991**, *113*, 3186.
(33) Sikora, D. J.; Moriarty, K. J.; Rausch, M. D.; Bulls, A. R.; Bercaw, J. E.; Patel, V. D.; Carty, A. J. *Inorg. Synth.* **1990**, *28*, 248.
(34) Fachinetti, G.; Floriani, C.; Chiesi-Villa, A.; Guastini, C. *J. Am. Chem. Soc.* **1979**, *101*, 1767.
(35) Harris, H. A.; Rae, A. D.; Dahl, L. F. *J. Am. Chem. Soc.* **1987**, *109*, 4739.
(36) X-ray structural analysis of the crystals isolated from the reaction of **1** with CS_2 showed them to have formed in a different habit to those isolated by Dahl *et al.* from the reaction of $Cp_2Ti(CO)_2$ with CS_2. X-ray data for $[Cp_2Ti]_2(C_2S_4)$: black tabular crystals, $P2_1/c$; $a = 8.5211(11)$ Å, $b = 8.4209(11)$ Å, $c = 14.2929(19)$ Å, $\beta = 95,889(10)°$, $V = 1020.2(4)$ Å^3; $d_{calc} = 1.66$ g cm^{-1} for $Z = 4$. Least-squares refinement of 1236 unique data with $F^2 > 3\sigma F^2$ collected at −97 °C with MoKα radiation converged at $R = 0.051$, $R_w = 0.083$.
(37) Samuel, E.; Rausch, M. D. *J. Am. Chem. Soc.* **1973**, *95*, 6263.
(38) (a) Wilkinson, G.; Cotton, F. A.; Birmingham, J. M. *J. Inorg. Nucl. Chem.* **1956**, *2*, 95. (b) Fischer, E. O.; Vigoureux, S. *Chem. Ber.* **1958**, *91*, 2205.
(39) Manzer, L. E. *J. Organomet. Chem.* **1976**, *110*, 291.
(40) Luetkens, M. L.; Sattleberger, A. P.; Murray, H. H.; Basil, J. D.; Fackler, J. P.; Jones, R. A.; Heaton, D. E. *Inorg. Synth.* **1990**, *28*, 305.
(41) Frajerman, C.; Meunier, B. *Inorg. Synth.* **1983**, *22*, 133.
(42) Burt, R. J.; Chatt, J.; Hussain, W.; Leigh, G. J. *J. Organomet. Chem.* **1979**, *182*, 203.

300 spectrometer with an inverse broad band probe operating at 94.69 MHz. The 90° pulse for a 0.2 M sample of **2** in C_6D_6 was 10 μs at 94.69 MHz, and the T_1 of this sample was measured at 10 ms. In a typical experiment using the AMX 300, initial location of the tellurium signal was achieved using a 90° pulse, an acquisition time of 60 ms, and a relaxation delay of 30 ms. The frequency window was varied throughout the range of known ^{125}Te NMR chemical shifts until the resonance was located. Once located, the sweep width was narrowed and the spectrum re-recorded to ensure the signal was not folded. Acquisition times were varied according to the line width of the signal. All samples are referenced to the absolute Ξ for Me_2Te[43] and are adjusted according to the operating ^{1}H frequency of the machine used in the experiment using corrections for solvent where necessary.

$Cp_2Ti[TeSi(SiMe_3)_3]_2$ (1). A solution of $(THF)_2LiTeSi(SiMe_3)_3$ (5.00 g, 9.50 mmol) in hexanes (15 mL) was added dropwise to a stirred solution of Cp_2TiCl_2 (1.18 g, 4.72 mmol), also in hexanes (25 mL). Immediately upon addition of the lithium salt the mixture became an intense purple color. The mixture was stirred for 6 h and the solvent removed under reduced pressure. The black residue was extracted into hexane (30 mL), concentrated, and cooled to -40 °C to give the product, in three crops, as a black crystalline solid (3.78 g, 86%) (mp 181–182 °C). IR: 1256 sh, 1244 s, 1017 w, 837 vs br, 689 m, 622 m cm^{-1}. ^{1}H NMR (400 MHz): δ 6.07 (s, 10H), 0.47 (s, 54H). ^{13}C{^{1}H} NMR (100 MHz, C_6D_6): δ 111.0, 2.8 . UV–vis (hexane, nm): λ_{max} 220 (55900); 309 (13900); 360 (9900); 810 (4000). Anal. Calcd for $C_{28}H_{64}Si_8Te_2Ti$: C, 36.2; H, 6.95. Found: C, 35.6; H, 6.90.

$Cp_2Zr[TeSi(SiMe_3)_3]_2$ (2). Method A: A mixture of Cp_2ZrCl_2 (1.66 g, 5.70 mmol) and $(THF)_2LiTeSi(SiMe_3)_3$ (6.00 g, 11.4 mmol) was suspended in hexanes (50 mL). The solution immediately became red and the color gradually darkened to crimson over a period of 6 h. The solvent was removed and the residue extracted into hexanes. Concentration of this solution followed by cooling to –40 °C gave the product as red needles (4.14 g, 75 %) (mp 204–205 °C).

Method B: Hexane (50 mL) was added to a mixture of Cp_2ZrMe_2 (0.50 g, 2.00 mmol) and $HTeSi(SiMe_3)_3$ (1.50 g, 4.00 mmol). After being stirred overnight at 50 °C the mixture was worked up as in method A to yield 1.50 g (77%) of product. IR: 1307 w, 1256 m, 1243 s, 1014 m, 836 s, 685 m, 621 m cm^{-1}. ^{1}H NMR (400 MHz, C_6D_6): δ 6.03 (s, 10H), 0.47 (s, 54H). ^{13}C{^{1}H} NMR (C_6D_6): δ 110.0, 2.39. UV–vis (hexane, nm): λ_{max} 220 (58300); 290 (14800); 528 (10400). EI/MS, 972 (M^+), 725 ($M^+ - Si(SiMe_3)_3$), 597 ($M^+ - TeSi(SiMe_3)_3$). Anal. Calcd for $C_{28}H_{64}Si_8Te_2Zr$: C, 34.6; H, 6.64. Found: C, 34.3; H, 6.67.

$Cp_2Hf[TeSi(SiMe_3)_3]_2$ (3). A mixture of Cp_2HfCl_2 (0.18 g, 0.47 mmol) and $(THF)_2LiTeSi(SiMe_3)_3$ (0.50 g, 0.95 mmol) suspended in pentane (40 mL) was stirred at ambient temperature for 8 h. Upon addition of solvent, the mixture turned red and then darkened gradually until it was maroon. The solvent was removed under vacuum and the deep red residue was extracted with pentane. Partial removal of solvent followed by cooling to –40 °C afforded the product as a red crystalline solid in 2 crops (0.37 g, 72%) (mp 194–195 °C). IR: 1016 m, 834 vs, br, 817 sh, 808 sh, 728 w, 685 m, 668w, 662 m, 302 m, 281 w, 274 m, 253 m br, 234 sh, 226 s, 214 s, 207 s, 199 vs cm^{-1}. ^{1}H NMR (400 MHz, C_6D_6): δ 5.98 (s, 10H), 0.47 (s, 54H). ^{13}C{^{1}H} NMR (C_6D_6): δ 109.2, 2.84. Anal. Calcd for $C_{28}H_{64}Si_8Te_2Hf$: C, 31.8; H, 6.09. Found: C, 32.0; H, 6.19. UV–vis (hexane, nm): λ_{max} 218 (55000); 251 (27400); 310 (6500); 474 (9900). EI/MS, 1060 (M^+), 813 ($M^+ - Si(SiMe_3)_3$), 685 ($M^+ - TeSi(SiMe_3)_3$).

$Cp'_2Ti[TeSi(SiMe_3)_3]_2$ (4). This preparation was identical with that used to synthesize **1** (1.46 g, 70%) (mp 183–185 °C). ^{1}H NMR (400 MHz, C_6D_6): δ 6.62 (t, J = 2.2 Hz, 2H), 5.95 (t, J = 2.4 Hz, 2H), 1.51 (s, 6H), 0.29 (s, 54H). ^{13}C{^{1}H} NMR (100 MHz, C_6D_6): δ 121.5, 115.1, 111.6, 16.7, 2.9. Anal. Calcd for $C_{28}H_{68}Si_8Te_2Ti$: C, 37.7; H, 7.11. Found: C, 37.5; H, 7.21.

$Cp_2Zr(Me)[TeSi(SiMe_3)_3]$ (5). A toluene solution of Cp_2ZrMe_2 (0.33 g, 1.3 mmol in 10 mL) was added to a cold (–78 °C) solution of $HTeSi(SiMe_3)_3$ (0.50 g, 1.3 mmol) in toluene (10 mL). The stirred solution was allowed to warm to room temperature. After 3 h the dark orange solution was evaporated under vacuum to give a dark red semisolid that was extracted with acetonitrile (2 × 15 mL). The solution was filtered, concentrated slightly, and cooled to –25 °C overnight. Orange-red plates of the product contaminated with ca. 5% of **2** were isolated by filtration. Attempts to purify the compound further were unsuccessful. ^{1}H NMR (300 MHz): δ 5.84 (s, 10H), 0.45 (s, 27H), –0.42 (s, 3H). EI MS, m/z: 612 (M^+).

(43) McFarlane, H. C. E.; McFarlane, W. In *Multinuclear NMR*; Mason, J., Ed.; Plenum: New York, 1987.

$Cp_2Zr[TeSi(SiMe_3)_3](\eta^2\text{-}COMe)$ (6). A toluene solution of Cp_2ZrMe_2 (0.33 g, 1.3 mmol in 10 mL) was added to a cold (–78 °C) solution of $HTeSi(SiMe_3)_3$ (0.50 g, 1.3 mmol) in the same solvent (10 mL). The stirred solution was allowed to warm to room temperature. After 2 h the dark orange solution was evaporated under vacuum to give a dark red semisolid that was extracted with hexane (20 mL) and transferred to a Fisher-Porter bottle. Shortly after the solution was pressurized with CO (40 psi), bright orange needles began to precipitate. Stirring was continued for 8 h after which time the product was filtered off in the form of an orange powder (0.50 g, 60%). Recrystallization from Et_2O gave bright orange needles (mp 147–150 °C). IR: 1551 s cm^{-1} (ν_{CO}). ^{1}H NMR (400 MHz, C_6D_6): δ 5.44 (s, 10H), 2.17 (s, 3H), 0.55 (s, 27H). ^{13}C{^{1}H} NMR (100 MHz, C_6D_6): δ 308.5, 110.0, 31.3, 2.20. Anal. Calcd for $C_{21}H_{40}OSi_4TeZr$: C, 39.4; H, 6.19. Found: C, 39.0; H, 6.40.

Reaction of Cp_2TiCl_2 with $(THF)_3LiTeC(SiMe_3)_3$. Cp_2TiCl_2 (6 mg, 24 μmol), $(THF)_3LiTeC(SiMe_3)_3$ (24 mg, 47 μmol), and Cp_2Fe (2 mg, 11 μmol, added as an internal standard) were mixed in a NMR tube fitted with a sealable Teflon cap. The tube and contents were cooled to –196 °C and C_7D_8 (0.6 mL) was added by vacuum transfer. The tube was warmed to –78 °C and transferred to the precooled (–60 °C) spectrometer probe. At this temperature the ^{1}H NMR spectrum showed only resonances assignable to starting materials and $HC(SiMe_3)_3$ [^{1}H NMR: δ 0.15 (s, 27 H), –0.89 (s, 1 H)]. Upon warming to –20 °C, the major soluble fragment was $HC(SiMe_3)_3$.

Reaction of Cp_2ZrCl_2 with $(THF)_3LiTeC(SiMe_3)_3$. Using a method analogous to that described above, Cp_2ZrCl_2 (64 mg, 14 μmol), $(THF)_3LiTeC(SiMe_3)_3$ (15 mg, 29 μmol), and Cp_2Fe (2 mg, 11 μmol) were mixed in an NMR tube which was cooled to –196 °C and C_7D_8 (0.6 mL) was added by vacuum transfer. The tube was warmed to –78 °C and transferred to the precooled (–60 °C) spectrometer probe, and the sample was warmed to –30 °C, at which stage, an intense red color developed. The ^{1}H NMR spectrum showed a mixture of **8** (57%) [^{1}H NMR: δ 5.89 (s, 10 H), 0.51 (s, 54 H)], $(THF_3)LiTeC(SiMe_3)$ (27%), and alkane (16%). The product, **8**, appeared stable at this temperature. Upon warming to room temperature, only $Cp_2Zr[C(SiMe_3)_3]_2$ (**10**) and alkane in a 2:1 ratio were observed.

$Cp_2Ti[TeSi(SiMe_3)_3](PMe_3)$ (11). Method A: A stirred hexane solution of **1** (1.00 g, 1.08 mmol) was treated with PMe_3 (0.45 mL, 4.35 mmol). The solution slowly turned red-brown over a period of 6 h. Removal of all volatiles under reduced pressure gave a brown solid, which was washed with cold HMDSO to remove $Te_2[Si(SiMe_3)_3]_2$. The remaining red powder was crystallized from hexanes giving the pure product as red needles in two crops (0.65 g, 96%).

Method B: A stirred suspension of $[Cp_2TiCl]_2$ (0.20 g, 0.56 mmol) in hexanes (25 mL) was treated with PMe_3 (0.12 mL, 1.16 mmol) and then a solution of $(THF)_2LiTeSi(SiMe_3)_3$ (5.9 g, 1.1 mmol) in hexane (10 mL). The color immediately became red-purple and the reaction mixture was stirred for 6 h. The solvent was removed and the residue was extracted with hexanes (3 × 15 mL). The combined filtrates were concentrated and placed at –20 °C to induce crystallization. Red needles (0.35 g, 50%) were obtained.

Method C: To a stirred THF solution (25 mL) of Cp_2TiCl_2 (0.25 g, 1.0 mmol) was added 150 μL (1.45 mmol) of PMe_3. Into this solution 1.07 g (2.03 mmol) of $(THF)_2LiTeSi(SiMe_3)_3$ in THF (20 mL) was added with an immediate color change to red-purple. After 1 h of stirring, workup as in method A yielded 0.36 g (57 %) of crystalline product. Mp 196 °C. IR: 1300 w, 1278 w, 1235 m, 1011 w, 945 m br, 863 sh, 830 s, br, 792 s, 721 m, 683 m, 618 m cm^{-1}. Anal. Calcd for $C_{22}H_{46}PSi_4TeTi$: C, 42.0; H, 7.32 Found: C, 42.0; H, 6.86. EI/MS, 375 ($TeSi(SiMe_3)_3^+$), 178 (Cp_2Ti^+), 76 (PMe_3^+). EPR (MCH, 298K): g_{iso} = 2.010 (ΔH = 3 G), $a_{iso}(^{31}P)$ = 20 G, $a_{iso}(^{47/49}Ti)$ = 10 G. μ_{eff} (Evan's method) = 1.6(1) μ_B.

$Cp_2Ti[TeSi(SiMe_3)_3](PEt_3)$ (12). Method A: In an analogous procedure to that used in method A above, **1** (0.60 g, 0.65 mmol) and PEt_3 (96 μL, 0.65 mmol) afforded 0.10 g (23%) of product.

Method B: $[Cp_2TiCl]_2$ (0.50 g, 1.2 mmol), $(THF)_2LiTeSi(SiMe_3)_3$ (1.23 g, 2.34 mmol), and PEt_3 (0.36 mL, 2.44 mmol) were combined in hexanes as described for **11** to yield 1.04 g (66%) of red needles. In both methods, multiple recrystallizations failed to eliminate a small impurity (5%) of **1**. ^{1}H NMR (400 MHz, C_6D_6): δ 1.60 (s br, 10H), 1.14 (s br, 27H).

$Cp_2Ti[TeSi(SiMe_3)_3](PMe_2Ph)$ (13). Method A: Dimethylphenylphosphine (92 μL, 0.65 mmol) was added to a stirred solution of **1** (0.60 g, 0.65 mmol) in hexanes (20 mL). The resulting mixture was stirred for 10 h by which time it had turned red-brown. An aliquot taken from this mixture showed the reaction to be incomplete and stirring was

continued for an additional 20 h, the hexanes was then removed under reduced pressure, leaving a brown tar which was left under dynamic vacuum for 4 h. The residue was extracted into pentane (10 mL) and crystallized at −40 °C. (Repeated recrystallizations from pentane afforded pure **13** (0.24 g, 54%).)

Method B: To a stirred suspension of $[Cp_2TiCl]_2$ (0.50 g, 1.2 mmol) in hexanes (10 mL) was added PMe_2Ph (0.40 mL, 0.39 g, 2.8 mmol) and a solution of $(THF)_2LiTeSi(SiMe_3)_3$ (1.24 g, 2.35 mmol) in hexanes (10 mL). Workup as above in method A yielded red-purple needles (1.36 g, 81%). ^1H NMR (400 MHz, C_6D_6): δ 8.85 (s br, 2H), 6.96 (s br, 1H), 1.24 (s br, 27H).

$Cp_2Ti[TeSi(SiMe_3)_3][(2,6\text{-}Me_2C_6H_3)NC]$ (14). Method A: A mixture of **1** (0.70 g, 0.75 mmol) and $(2,6\text{-}Me_2C_6H_3)NC$ (0.10 g, 0.76 mmol) in hexanes (40 mL) was stirred for 5 h at room temperature. The solvent was removed leaving a purple residue that was washed with cold HMDSO and then extracted into hexanes (20 mL). Concentration of the solution followed by cooling to −20 °C gave 0.36 g of purple plates. A second crop (0.13 g) was obtained from the supernatant (95%).

Method B: To a suspension of $[Cp_2TiCl]_2$ (0.25 g, 0.58 mmol) and $(2,6\text{-}Me_2C_6H_3)NC$ (0.15 g, 1.2 mmol) in hexanes (20 mL) was added a hexanes solution (20 mL) of $(THF)_2LiTeSi(SiMe_3)_3$ (0.62 g, 1.2 mmol). After the solution was stirred for 4 h, the volatile materials were removed under vacuum and the residue was extracted with hexanes (2 × 15 mL). Reduction of the extracts followed by crystallization at −40 °C afforded 0.74 g (93 %) of purple plates. Mp 159–160 °C. IR: 1936 cm^{-1} (ν_{NC}). ^1H NMR (400 MHz, C_6D_6): δ 1.31 (s br). Anal. Calcd for $C_{28}H_{46}N_1Si_4Te_1Ti$: C, 49.1; H, 6.59. Found: C, 48.9; H, 6.59. UV–vis (hexane): λ_{max} 550 nm. EI/MS, 551 (M^+ − $(2,6\text{-}Me_2C_6H_3)NC$, 131 ($(2,6\text{-}Me_2C_6H_3)NC$). EPR (MCH, 298K): g_{iso} = 2.027. (ΔH = 7 G). μ_{eff}(Evan's method) = 1.6(1) μ_B.

Reaction of 1 with CO. A Fisher-Porter bottle containing a solution of **1** (0.41 g, 0.44 mmol) in hexanes (20 mL) was charged with CO (1 atm) and stirred at 50 °C for 14 h. Within 30 min, the black mixture had become dark green. The solvent was removed under reduced pressure and the residue extracted with HMDSO. An aliquot of this residue showed the product to be $Cp_2Ti(CO)_2$ by comparison of its IR and NMR spectra with reported spectra. Isolation of pure $Cp_2Ti(CO)_2$ was hindered by co-crystallization of $Te_2[Si(SiMe_3)_3]_2$.

Reaction of 1 with CO_2. To a Fisher-Porter bottle charged with a solution of **1** (1.00 g, 1.08 mmol) in toluene (40 mL) was added CO_2 (1 atm). The resulting mixture was stirred for 36 h at 60 °C over which time the reaction mixture turned green and a lime green solid precipitated.

The toluene was removed under reduced pressure and the volatiles were bubbled through a solution of Cp_2V in hexanes. Formation of $Cp_2V(CO)$ (ν 1896 cm^{-1}) confirmed the presence of CO. The residue was washed with hexanes to remove $[TeSi(SiMe_3)_3]_2$ and the remaining green residue was recrystallized from toluene to give 125 mg of $\{[Cp_2Ti]_2(CO_3)\}_2$ (57%), whose authenticity was checked by comparison with literature values.[34]

Reaction of 1 with CS_2. A solution of **1** (0.50 g, 0.54 mmol) in benzene (20 mL) was treated with CS_2 (5 mL, 6.33 g, 56.7 mmol). The reaction mixture was allowed to stand for 2 days at room temperature by which time dark purple crystals had formed in near quantitative yield. Analysis of the product showed it to be identical with that reported by Dahl *et al.* for $[(Cp_2Ti)_2(C_2S_4)]$.[35]

X-ray Crystallographic Studies. The structures of **2**, **6**, and **11** were determined by Dr. F. J. Hollander at the University of California College of Chemistry X-ray facility (CHEXRAY).

2: Dark red plate-like crystals were obtained by slow crystallization from pentane at −40 °C. A fragment of one of these crystals was mounted on a glass fiber using Paratone-N hydrocarbon oil. The crystal was transferred to an Enraf-Nonius CAD-4 diffractometer, centered in the beam, and cooled to −108 °C by a nitrogen-flow low-temperature apparatus which had been previously calibrated by a thermocouple placed at the same position as the crystal. Automatic peak search and indexing procedures yielded an orthorhombic reduced primitive cell. Inspection of the Niggli values revealed no conventional cell of higher symmetry. Inspection of the systematic absences indicated uniquely space group *Pnna*. The 6649 raw intensity data were converted to structure factor amplitudes and their esd's by correction for scan speed, background, and Lorentz and polarization effects. Removal of the systematically absent data and averaging of redundant data left 3052 unique data in the final data set. In a difference Fourier map calculated following the refinement of all non-hydrogen atoms with anisotropic thermal parameters, peaks were found corresponding to the positions of most of the hydrogen atoms. Hydrogen atoms were assigned idealized locations and values of B_{iso} approximately 1.2 times the B_{eqv} of the atoms to which they were attached. They were included in structure factor calculations but not refined.

4: Large block-like crystals were obtained by slow crystallization from pentane at −15 °C. A fragment obtained from one of these crystals was mounted, centered, and cooled to −100 °C as described above. The unit cell was determined to be centric monoclinic and subsequent examination of systematic absences in the data set indicated the space group $C2/c$. The 3448 raw intensity data were reduced to 3141 unique data in the final set using procedures outlined above. Most of the hydrogen atoms were located in a difference Fourier map following anisotropic refinement of all non-hydrogen atoms. Hydrogen atoms were assigned idealized locations and values of B_{iso} approximately 1.2 times the B_{eqv} of the atoms to which they were bonded. They were included in structure factor calculations but not refined.

6: Large yellow plate-like crystals were obtained by slow crystallization from Et_2O at −40 °C. A fragment obtained from one of these crystals was mounted, centered, and cooled to −110 °C on the diffractometer as described above. The unit cell was determined to be primitive monoclinic and subsequent examination of systematic absences in the data set indicated uniquely space group $P2_1/c$. Conversion of the 8514 raw intensity data to structure factor amplitudes and their esds as described above followed by removal of systematic absences and redundant data left 7755 unique data in the final set. Nearly all hydrogen atoms were located in a difference Fourier map following anisotropic refinement of all non-hydrogen atoms. Hydrogen atoms were assigned idealized locations and values of B_{iso} approximately 1.15 times the B_{eqv} of the atoms to which they were bonded. They were included in structure factor calculations but not refined. In the final cycles of refinement a secondary extinction parameter was included (maximum correction was 0.05 on F). Also, 58 data showed exceptionally bad agreement and were given zero weight.

11: Dark red needle-like crystals of the compound were obtained by slow crystallization from pentane at −40 °C. A fragment from one of these crystals was mounted on a glass fiber using Paratone-N hydrocarbon oil, transferred to the diffractometer, cooled to −98 °C, and centered as described previously. Automatic peak searching yielded a monoclinic, reduced primitive cell. Inspection of the Niggli values revealed no convention cell of higher symmetry. Following inspection of systematic absences, space group $P2_1/a$, a non-standard form of $P2_1/c$, was indicated uniquely. The 8644 raw data were reduced to 8204 unique data and used in the final data set. Hydrogen atoms were assigned idealized locations and values of B_{iso} 1.25 times the B_{eqv} of the atoms to which they were bonded. They were included in structure factor calculations but not refined. In the final cycles of least-squares refinement 144 data which were apparently affected by the presence of a second crystal in the sample (all $F_o \gg F_c$ and flagged with offset peaks in the output) were given zero weight. Inspection of the residuals ordered in ranges of $\sin\theta/\lambda$, $|F_o|$, and parity and value of the individual indexes showed that weak reflections with $h + l$ odd were significantly more poorly fit than others, otherwise there were no other unusual features or trends.

Acknowledgment. We thank the National Science Foundation for financial support and Wayne Lukens and Dr. Norman Edelstein for their help with EPR spectroscopy. S.P.W. is grateful to the Department of Education for a graduate student fellowship.

Supplementary Material Available: Tables of temperature factor expressions, positional parameters, intramolecular distances and angles, least-squares planes, and anisotropic thermal parameters (42 pages); listings of observed and calculated structure factors (129 pages). Ordering information is given on any current masthead page.